JOURNAL OF GUIDANCE, CONTROL, AND DYNAMICS
Vol. 34, No. 4, July–August 2011

Engineering Notes

Quantitative Performance for Spacecraft Rendezvous Trajectory Safety

Ya-zhong Luo,* Li-bo Liang,† Hua Wang,‡ and Guo-jin Tang§
National University of Defense Technology, 410073 Changsha, People's Republic of China

DOI: 10.2514/1.52041

I. Introduction

SAFETY requirements are some of the most critical aspects of the definition of an operational profile for a rendezvous mission [1]. Numerous methods for generating safe rendezvous trajectories have been reported in the literature. Early representative work in this regard can be found in [2,3]. Hechler [2] proposed a method of linear optimization for minimum-fuel rendezvous that considers the constraints of collision avoidance if the chaser is operating out of control. Eckstein [3] proposed an approach that is based on the Clohessy–Wiltshire (C–W) equations for the design of approach trajectories toward an orbiting space station, with an emphasis on safety aspects. Recently, Roger and McInnes [4] planned passively safe trajectories using potential functions. Jacobsen et al. [5] presented a numerical optimization method that employs both safety and fuel as optimization objectives in the planning of a safe spatial trajectory of a robot capturing an uncontrolled spinning satellite. This method was also applied by Matsumoto et al. [6]. Fehse [1] and Naasz [7] developed the safety ellipse method for the analysis of safe approach trajectories. More recently, Breger and How [8] proposed a method for the onboard generation of safe fuel-optimized rendezvous trajectories that guarantee collision avoidance for a large class of anomalous system behaviors. They also examined the tradeoffs between passive and active approaches to safety.

For the design of safe rendezvous trajectories, the analysis of safety performance is both significant and essential. However, few studies have addressed the quantitative analysis of safety performance [5,8]. It is more difficult to quantify the safety of an approach trajectory than to quantify conventional performance metrics, such as fuel usage or time. There are many possible measures of safety during approach, such as distance to the target, time within an area close to the target, and probability of collision. In [5], the measure of safety for a given point along a trajectory was the time to collision with the satellite beginning with the point at which the robot's thrusters failed. In another approach [8], the probability of the collision metrics was employed, which is defined as the probability of failure at any time step during a maneuver that results in a collision between the target and the chaser spacecraft. Recently, Luo et al. [9–11] defined the minimum distance between the chaser and the target in the chaser's free-flying path as the trajectory safety performance index, and they completed the multiobjective optimization design of an impulsive rendezvous that includes the minimum characteristic velocity, minimum flight duration, and maximum safety performance index.

However, the preceding studies on safety performance focus mainly on a normal trajectory, without considering operational error. In the design of a practical rendezvous trajectory, the navigation, control, and guidance errors that may arise in all phases of the rendezvous must be taken into consideration. The main goal of this study is to determine a quantitative performance index of safety factors for spacecraft rendezvous trajectories that considers both navigation and control errors. This safety performance index involves the minimum distance between the 3σ ellipsoid of the chaser and the control zone of the target, in addition to the maximum probability of instantaneous collision between these two spacecraft. The purpose of the former (minimum distance) is to quantify the degree of safety under the condition of no intersection between the 3σ ellipsoid and the control zone, whereas the purpose of the latter (maximum collision probability) is to quantify the probability of collision when they intersect.

This Note provides a detailed definition of this performance index. It also presents several attempts made to accelerate the method of safety performance analysis for trajectory design. In addition, the effectiveness and efficiency of the performance index are verified using the example of a simulation. Finally, the different influences of transfer time, number of impulses, and intervals between impulses on the trajectory's safety characteristics are analyzed.

II. Rendezvous Trajectory Safety Description

A rendezvous mission can be divided into a number of major phases: launch, phasing, far-range rendezvous (homing rendezvous), close-range rendezvous, and mating [1]. The discussions on trajectory safety concentrate on the rendezvous phases, because the mission phases of launch and phasing are generally controlled by operators or computer functions on the ground. In general, two categories of rendezvous trajectory safety are considered: active trajectory protection and passive trajectory protection. Active trajectory protection focuses on the design of an approximate active collision-avoidance maneuver; more details on this issue can be found in [1]. Passive trajectory protection, on the other hand, focuses on the design of all trajectory elements to create an approach trajectory sequence such that, if at any point in the trajectory thrust control ceases, the resulting free trajectory will remain collision free for a time to be determined (TBD). In this study, only passive trajectory protection is considered.

To guarantee the safety of a rendezvous mission, the volumes around the target spacecraft, particularly around space stations with their large and complex structures, are defined, and visiting spacecraft are subject to certain rules within these volumes. In such control zones, the hierarchy of control authority of the parties involved, the maximum Δv allowed, operational procedures that are determined, and the approach and departure corridors may be defined. As an example, the control zones and approach/departure corridors of the International Space Station (ISS) are shown in Fig. 1 [1]. The outer zone, called the approach ellipsoid (AE), has an extension of ± 2000 m in the V-bar direction and ± 1000 m in the other directions. Before entering the AE, overall control authority is taken over by the ISS control center. The inner control zone, the so-called keepout sphere (KOS), is a sphere with a radius of 200 m that can be entered only through one of the approach or departure corridors.

Presented as Paper 2010-7662 at the AIAA/AAS Astrodynamics Specialist Conference, Toronto, 2–5 August 2010; received 19 August 2010; revision received 6 March 2011; accepted for publication 11 March 2011. Copyright © 2011 by the American Institute of Aeronautics and Astronautics, Inc. All rights reserved. Copies of this Note may be made for personal or internal use, on condition that the copier pay the $10.00 per-copy fee to the Copyright Clearance Center, Inc., 222 Rosewood Drive, Danvers, MA 01923; include the code 0731-5090/11 and $10.00 in correspondence with the CCC.

*Associate Professor, College of Aerospace and Materials Engineering; luoyz@nudt.edu.cn. Senior Member AIAA (Corresponding Author).

†Ph.D. Candidate, College of Aerospace and Materials Engineering; rachel_libo@hotmail.com.

‡Lecturer, College of Aerospace and Materials Engineering; wanghua21cn@21cn.com.

§Professor, College of Aerospace and Materials Engineering; tanggj@nudt.edu.cn.

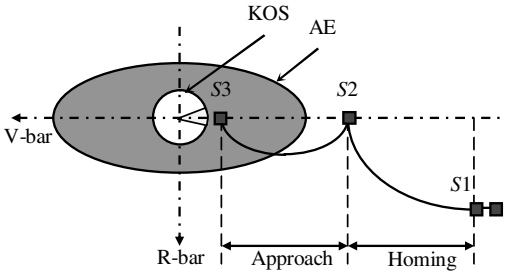

Fig. 1 Control zones of ISS.

In the approach process, it must be guaranteed that the chaser does not enter the control zone of the target with any trajectory dispersions [1]. The trajectory dispersions of the chaser can be described by the 3σ ellipsoid of positions. Thus, the problem of approach trajectory safety can be expressed as a problem that involves analysis of the potential collision between the 3σ ellipsoid of the chaser and the control zone of the target. In the following sections, a model for calculating the 3σ ellipsoid is first provided, and then the performance index for trajectory safety associated with the 3σ ellipsoid and the control zone is defined.

III. Error Propagation Model

A. Dynamic Model

The relative dynamic motion for rendezvous is illustrated by the C–W equations, which are set up in the local-vertical local-horizontal (LVLH) frame. The LVLH frame has its origin at the target's center of mass and is a right-handed Cartesian coordinate frame, with the x axis along the target velocity vector, the z axis radially downward to the Earth's center of mass, and with the y axis completing the right-handed frame:

$$\begin{cases} \ddot{x} - 2\omega\dot{z} = u_x \\ \ddot{y} - \omega^2 y = u_y \\ \ddot{z} + 2\omega\dot{x} - 3\omega^2 z = u_z \end{cases} \tag{1}$$

where $\mathbf{X} = (x \quad y \quad z \quad \dot{x} \quad \dot{y} \quad \dot{z})^T = (\mathbf{r} \quad \mathbf{v})^T$ is the relative state vector of the chaser, ω is the orbital angular velocity of the target, and $\mathbf{U} = [u_x \quad u_y \quad u_z]^T$ is the thrust acceleration vector acting on the chaser in the LVLH frame.

The solution to the C–W equations can be written in the form

$$\mathbf{X}(t) = \mathbf{\Phi}(t, t_0)\mathbf{X}_0 + \int_{t_0}^{t} \mathbf{\Phi}_v(t, s)\mathbf{U}(s)\,\mathrm{d}s \tag{2}$$

and the transition matrix $\mathbf{\Phi}(t, t_0)$ is given by

$$\mathbf{\Phi}(t, t_0) = \begin{bmatrix} 1 & 0 & 6(\tau - \sin\tau) & \frac{4\sin\tau - 3\tau}{\omega} & 0 & \frac{2(1-\cos\tau)}{\omega} \\ 0 & \cos\tau & 0 & 0 & \frac{\sin\tau}{\omega} & 0 \\ 0 & 0 & 4 - 3\cos\tau & \frac{2(\cos\tau - 1)}{\omega} & 0 & \frac{\sin\tau}{\omega} \\ 0 & 0 & 6\omega(1 - \cos\tau) & 4\cos\tau - 3 & 0 & 2\sin\tau \\ 0 & -\omega\sin\tau & 0 & 0 & \cos\tau & 0 \\ 0 & 0 & 3\omega\sin\tau & -2\sin\tau & 0 & \cos\tau \end{bmatrix} \tag{3}$$

where $\tau = \omega(t - t_0)$. $\mathbf{\Phi}(t, t_0)$ can be divided into two 6×3 matrices:

$$\mathbf{\Phi}(t, t_0) = [\mathbf{\Phi}_{\mathbf{r}}(t, t_0) \quad \mathbf{\Phi}_{\mathbf{v}}(t, t_0)] \tag{4}$$

Supposing that there are n impulse maneuvers $\mathbf{\Delta v_i}(i = i, \ldots, n)$ applied at t_i during the rendezvous process, the state vector at any time t $(t_0 \le t \le t_f)$ is given by

$$\mathbf{X}(t) = \mathbf{\Phi}(t, t_0)\mathbf{X}_0 + \sum_{i=1}^{i=j} \mathbf{\Phi}_{\mathbf{v}}(t, t_i)\mathbf{\Delta v_i} \tag{5}$$

where $\mathbf{\Delta v}_j$ at t_j $(j \le n)$ is the last impulse before time t.

B. Error Covariance Propagation

In this study, the navigation and control errors are considered and the linear covariance method is adopted to propagate the errors.

The model for initial navigation error is

$$\mathbf{X}'_0 = \mathbf{X}_0 + \delta\mathbf{X}_0 \tag{6}$$

where $\delta\mathbf{X}_0$ is an independent white error and each component is zero-mean white noise.

The error model for an impulse vector is assumed as follows:

$$\Delta\mathbf{v}'_{\mathbf{i}} = \Delta\mathbf{v_i} + \delta\Delta\mathbf{v}_i \tag{7}$$

where $\delta\Delta\mathbf{v_i}$ is an impulse error for which the error model is assumed to be a zero-mean white noise process.

Substituting Eqs. (6) and (7) into Eq. (5), the final state errors are defined by

$$\delta\mathbf{X} = \mathbf{\Phi}(t, t_0)\delta\mathbf{X}_0 + \sum_{i=1}^{i=j} \mathbf{\Phi}_{\mathbf{v}}(t, t_i)\delta\mathbf{\Delta v_i} \tag{8}$$

It should be noted that

$$\delta\Delta\mathbf{v} = [(\delta\Delta\mathbf{v}_1)^T \quad (\delta\Delta\mathbf{v}_2)^T \quad \cdots \quad (\delta\Delta\mathbf{v}_j)^T]^T \tag{9}$$

$$\mathbf{F} = [\mathbf{\Phi}_{\mathbf{v}}(t, t_1) \quad \mathbf{\Phi}_{\mathbf{v}}(t, t_2) \quad \cdots \quad \mathbf{\Phi}_{\mathbf{v}}(t, t_j)] \tag{10}$$

The mean value of $\delta\mathbf{X}$ is

$$\mathbf{E}(\delta\mathbf{X}) = \mathbf{E}(\mathbf{\Phi}(t, t_0)\delta\mathbf{X}_0 + \sum_{i=1}^{i=j} \mathbf{\Phi}_{\mathbf{v}}(t, t_i)\delta\mathbf{\Delta v_i}) = 0 \tag{11}$$

$\mathbf{C}_{\delta\mathbf{X}_0}$ and $\mathbf{C}_{\delta\mathbf{\Delta v}}$ are considered as covariance matrices of the initial navigation errors and control errors, respectively, and the covariance matrix with respect to $\delta\mathbf{X}$ is then obtained as

$$\mathbf{C}_{\delta\mathbf{X}} = \mathbf{E}\{[\delta\mathbf{X} - \mathbf{E}(\delta\mathbf{X})][\delta\mathbf{X} - \mathbf{E}(\delta\mathbf{X})]^T\} = \mathbf{\Phi}(t, t_0)\mathbf{C}_{\delta\mathbf{X}_0}\mathbf{\Phi}(t, t_0)^T + \mathbf{F}\mathbf{C}_{\delta\mathbf{\Delta v}}\mathbf{F}^T \tag{12}$$

$\mathbf{C}_{\delta\mathbf{X}}$ can be divided into four 3×3 matrices:

$$\mathbf{C}_{\delta\mathbf{X}} = \begin{bmatrix} \mathbf{C_r} & \mathbf{C_{rv}} \\ \mathbf{C_{vr}} & \mathbf{C_v} \end{bmatrix} \tag{13}$$

The trajectory safety at time t is mainly influenced by the relative position and its errors. Thus, the covariance matrix of the position errors $\mathbf{C_r}$ is the main element of concern of $\mathbf{C}_{\delta\mathbf{X}}$.

To calculate the 3σ ellipsoid with respect to the relative position error, a technique based on an eigenvalue-eigenvector decomposition of the covariance is employed [12].

Let

$$\mathbf{M}^T\mathbf{C_r}\mathbf{M} = \mathbf{A} \tag{14}$$

where the diagonal matrix $\mathbf{A}$ contains the eigenvalues of $\mathbf{C_r}$, and the columns of $\mathbf{M}$ contain the corresponding eigenvectors. $\mathbf{M}^T$ is a transformation matrix that is from the LVLH frame to that defined by the principal axes of the ellipsoid.

The eigenvalues of $\mathbf{C_r}$ are obtained using Eq. (14), which are employed to determine the squared dimensions of the 1σ surface of the covariance ellipsoid [12]. Therefore, the 3σ ellipsoid with respect to the relative position error of the chaser can be determined and then used to describe the trajectory dispersions.

IV. Definition and Calculation of Quantitative Performance

A. Definition of Performance

Following the definition of passive safety, the trajectory safety, including trajectory uncertainties, can be described by the relationship between the 3σ ellipsoid of the chaser and the control zone of the target in a TBD time after arbitrary cessation of the rendezvous process.

The relationship between the chaser and the target at any time is illustrated in Fig. 2. As shown in Fig. 2a, when there is no collision between the 3σ ellipsoid of the chaser and the control zone of the target, the minimum distance between them, denoted as R_{rel}, is adopted to quantify the degree of safety. In Fig. 2b, when there is an encounter between them, R_{rel}, which is equal to zero, cannot quantify the degree of danger. Instead, the instantaneous collision probability between the two spacecraft, denoted as p_c, is introduced in order to quantify the degree of danger. Therefore, the quantitative performance index for the safety between two spacecraft for a TBD time, called $I_{\text{safe}}^{\text{TBD}}$, is defined as

$$I_{\text{safe}}^{\text{TBD}} = \begin{cases} \max\limits_{\text{TBD}}(-R_{\text{rel}}), & {}^{R_{\text{rel}}>0}_{\text{TBD}} \\ \max\limits_{\text{TBD}}(p_c), & R_{\text{rel}} = 0 \end{cases} \tag{15}$$

To describe the safety of a passive trajectory, every point in the rendezvous process should be evaluated. However, considering that the trajectory of the chaser between successive impulses is free, only the initial point and the n impulse points, i.e., $t_i (i = 0, 1, \ldots, n)$, are chosen as evaluation points to determine $I_{\text{safe}}^{\text{TBD}}(t_i)$. Herein, I_{safe}, which denotes the safety performance of the entire rendezvous trajectory, is defined as

$$I_{\text{safe}} = \max[I_{\text{safe}}^{\text{TBD}}(t_0), I_{\text{safe}}^{\text{TBD}}(t_1), \ldots, I_{\text{safe}}^{\text{TBD}}(t_n)] \tag{16}$$

B. Minimum Distance

The first part of the quantitative performance index of safety for spacecraft rendezvous trajectories, including uncertainty, is defined as the minimum distance between the 3σ ellipsoid of the chaser and the control zone of the target.

1. *Algorithm for Point (Algorithm 1)*

The minimum distance between the 3σ ellipsoid of the chaser and the control zone of the target at time τ is defined as $d(\tau)$. The calculation of $d(\tau)$ includes the following two main processes (steps):

Step 1: Prejudgment.

Step 1.1: Suppose that the 3σ ellipsoid of the chaser is ellipsoid E_1 with major axes (a_1, b_1, c_1) and the control zone of the target is ellipsoid E_2 with major axes (a_2, b_2, c_2). Here, the principle axes (a_1, b_1, c_1) of E_1 change as time goes by, while the principle axes (a_2, b_2, c_2) of E_2 do not change; and the major axis a_2 is along with the x axis of the LVLH frame, and b_2 is along with the z axis of the LVLH frame.

Step 1.2: Calculate the distance between the centers of the ellipsoids, denoted as r_{cc}.

Step 1.3: If

$$r_{cc} \le \min(a_1, b_1, c_1) + \min(a_2, b_2, c_2)$$

$d(\tau) = 0$. Otherwise, go to step 2.

Step 2: Calculate the minimum distance between E_1 and E_2 [13].

Step 2.1: The principle axis frame of E_1 is called frame A, and that of E_2 is known as the control zone attached to the target in LVLH frame. The transformation matrix from the LVLH frame to frame A is $\mathbf{M}^T$, as obtained by Eq. (14).

Step 2.2: Choose an arbitrary point P_1 on the surface of E_1 and define the position vector $\mathbf{r}_{E_2}$ of P_1 in the LVLH frame.

Step 2.3: Calculate $\mathbf{r}_{E_2}^T \mathbf{D}_2 \mathbf{r}_{E_2}$. If $\mathbf{r}_{E_2}^T \mathbf{D}_2 \mathbf{r}_{E_2} < 1$, point P_1 is inside E_2, then end. Otherwise, go to step 2.4. Here, $\mathbf{D}_2$ is defined by

$$\mathbf{D}_2 = \begin{bmatrix} 1/a_2^2 & 0 & 0 \\ 0 & 1/b_2^2 & 0 \\ 0 & 0 & 1/c_2^2 \end{bmatrix} \tag{17}$$

Step 2.4: Determine the minimum distance r_{12} from point P_1 to E_2, and obtain the corresponding point P_2 on the surface of E_2. The position vector of P_2 in the LVLH frame is denoted as $\mathbf{r}_{p_2}$.

Step 2.5: Calculate the position vector $\mathbf{r}_{E_1}$ of P_2 in frame A,

$$\mathbf{r}_{E_1} = \mathbf{M}^T \mathbf{r}_{p_2} \tag{18}$$

and then calculate $\mathbf{r}_{E_1}^T \mathbf{D}_1 \mathbf{r}_{E_1}$. If $\mathbf{r}_{E_1}^T \mathbf{D}_1 \mathbf{r}_{E_1} < 1$, point P_2 is inside E_1, then end. Otherwise, go to step 2.6. Here, $\mathbf{D}_1$ is defined by

$$\mathbf{D}_1 = \begin{bmatrix} 1/a_1^2 & 0 & 0 \\ 0 & 1/b_1^2 & 0 \\ 0 & 0 & 1/c_1^2 \end{bmatrix} \tag{19}$$

Step 2.6: Determine the minimum distance r_{21} from point P_2 to E_1, and obtain the corresponding point P_1 on the surface of E_1.

Step 2.7: Repeat steps 2.3–2.6 until $|r_{12} - r_{21}| < 1.0\text{e}-8$. Furthermore, if the number of iterations is larger than the predefined maximum number (50 in this study), then end.

2. *Algorithm for To-Be-Determined Time (Algorithm 2)*

Assume that the rendezvous time is from t_0 to t_f and that thrust control ceases at time τ_0 ($t_0 \le \tau_0 \le t_f$). The minimum value of $d(\tau)$ in the entire TBD time is used to measure the safety of the drift trajectory of the chaser after τ_0 and is defined as

$$d_{\min}(\tau_0) = \min_{\tau_0 \le \tau \le \tau_0 + \text{TBD}} d(\tau) \tag{20}$$

The process for calculating $d_{\min}(\tau_0)$ is given as follows:

Step 1: Define step as the calculation step, and let $k = 0$.

Step 2: $\tau = \tau_0 + k * \text{step}$.

Step 3: Calculate $d(\tau)$.

Step 3.1: Calculate the mean value of $\mathbf{X}(\tau)$ and the covariance matrix with respect to $\delta\mathbf{X}(\tau)$.

Step 3.2: Calculate the 3σ ellipsoid.

Step 3.3: Determine $d(\tau)$ using Algorithm 1.

Step 4: If $\tau \ge \tau_0 + \text{TBD}$, go to step 5. Otherwise, $k+ = 1$; go to step 2.

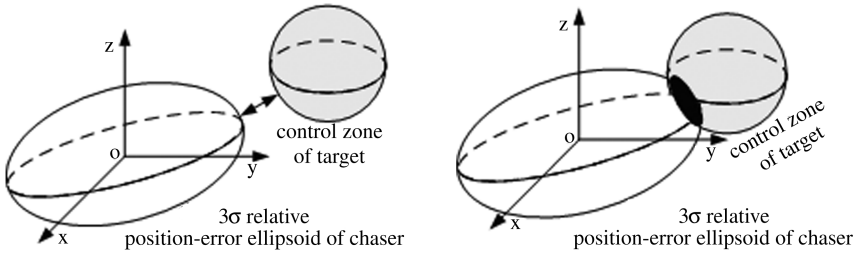

a) Safety **b) Danger**

Fig. 2 Rendezvous safety performance with uncertainty.

Step 5:

$$d_{\min}(\tau_0) = \min[d(\tau_0), d(\tau_0 + \text{step}), \ldots, d(\tau_0 + \text{TBD})]$$

3. Simplified Algorithm for To-Be-Determined Time (Algorithm 3)

In Algorithm 2, because the $d(\tau)$ value of every point in the range of $[\tau_0, \tau_0 + \text{TBD}]$ must be calculated, expensive computation is inevitable. To improve the efficiency of Algorithm 2, a simplified method is employed. This simplified algorithm is as follows:

Step 1: Calculate the minimum relative distance between the chaser and target in the range of $[\tau_0, \tau_0 + \text{TBD}]$ by employing the algorithm in [9] to obtain the corresponding time $\tau_{\min}$.

Step 2: Calculate $d(\tau_{\min})$ and let $d_{\min}(\tau_0) = d(\tau_{\min})$.

C. Maximum Collision Probability

The second part of the quantitative performance index of safety for spacecraft rendezvous trajectories, including uncertainty, is defined as the maximum probability of instantaneous collision between two spacecraft.

1. Algorithm for Point (Algorithm 4)

The probability of collision between the chaser and the target at arbitrary time τ is defined as $p(\tau)$. The variable $p(\tau)$ is obtained by a three-dimensional (3-D) integral [14]:

$$p(\tau) = \frac{1}{\sqrt{(2\pi)^3|\mathbf{C_r}|}} \iiint_{\text{volume}} \exp\left(-\frac{1}{2}\mathbf{r}^T\mathbf{C}_\mathbf{r}^{-1}\mathbf{r}\right) \mathrm{d}x\,\mathrm{d}y\,\mathrm{d}z = \iiint_{\text{volume}} f(\mathbf{r})\,\mathrm{d}x\,\mathrm{d}y\,\mathrm{d}z \tag{21}$$

where $f(\mathbf{r})$ is a 3-D Gaussian probability density function (PDF) with respect to position errors, and the integral volume is considered as an envelope sphere. Its radius is equal to the radius of the envelope sphere of the chaser plus that of the target.

2. Simplified Algorithm for Point (Algorithm 5)

If the PDFs are distributed evenly in the integral volume, $p(\tau)$ can be calculated using only the PDF of the center point denoted as $f(\mathbf{r}_c)$:

$$p(\tau) = f(\mathbf{r}_c)^* U_{\text{vol}} \tag{22}$$

where U_{vol} is the volume of the integral volume.

3. Algorithm for To-Be-Determined Time (Algorithm 6)

Similar to the approach in the minimum distance analysis method, the rendezvous time is assumed from t_0 to t_f and thrust control ceases at time τ_0 ($t_0 \le \tau_0 \le t_f$). The maximum value of $p(\tau)$ in the TBD time after τ_0 is employed to measure the safety of the drift trajectory of the chaser as follows:

$$p_{\max}(\tau_0) = \max_{\tau_0 \le \tau \le \tau_0 + \text{TBD}} p(\tau) \tag{23}$$

With Eq. (23), the process for calculating $p_{\max}(\tau_0)$ is similar to the calculation of $d_{\min}(\tau_0)$ in Algorithm 2.

4. Simplified Algorithm for To-Be-Determined Time (Algorithm 7)

As in Algorithm 3, a simplified method is employed to improve the efficiency of Algorithm 6 as follows:

Step 1: Calculate the maximum PDF of the center point in the range of $[\tau_0, \tau_0 + \text{TBD}]$ and obtain the corresponding time $\tau_{\max}$.

Step 2: Calculate $p(\tau_{\max})$ and let $p_{\max}(\tau_0) = p(\tau_{\max})$.

Algorithm 1 is based upon one proposed by Coppola and Woodburn [13], which has been widely employed and tested with good convergence properties (via simulation but not analytically proven) [15]. Algorithms 2–3 both employ Algorithm 1 to obtain the minimum value using an approximate method, and they also display good convergence properties in practice. Algorithm 4 uses only quadrature with smooth functions as integrands; Algorithms 5–7 are all approximate approaches based on Algorithm 4, guaranteeing their convergence.

V. Example

In this section, an example of a homing rendezvous mission is studied to confirm the efficiency and effectiveness of the performance index of safety and its simplified calculation method.

A. Problem Configuration

Assume that the target orbit is a 400 km circular orbit. The initial relative state of the chaser spacecraft is

$$\mathbf{X}_0 = (-20{,}000\ \text{m},\quad 400\ \text{m},\quad 2000\ \text{m},\quad 8\ \text{m/s},\quad 0,\quad -1\ \text{m/s})^T$$

and the terminal conditions are $t_f = 3200$ s,

$$\mathbf{X}_f = (-400\ \text{m},\quad 0,\quad 0,\quad 0,\quad 0,\quad 0)^T$$

The covariance matrix with respect to the initial navigation errors of the chaser is

$$\mathbf{C}_{\delta\mathbf{X}_0} = \text{diag}(100, 100, 100, 0.01, 0.01, 0.01)$$

The covariance matrix with respect to control errors is

$$\mathbf{C}_{\delta\mathbf{\Delta v_i}} = \text{diag}[(0.02 + 0.01\Delta v_i)^2, (0.02 + 0.01\Delta v_i)^2, (0.02 + 0.01\Delta v_i)^2]$$

The control zone of the target spacecraft is a sphere with a 200 m radius, and the integral volume of $p(\tau)$ is a sphere with a 100 m radius.

The normal maneuver impulses are listed in Table 1. According to Eq. (16), the four evaluation points that are selected are the states at 0, 500, 1500, and 3000 s.

B. Performance Calculation Results

Table 2 lists the results for the four evaluation points, including the time for the minimum distance between spacecraft centers ($t_{\min\text{-}d\text{-center}}$), the time for the minimum distance between the 3σ ellipsoid and the control zone ($t_{\min\text{-}d\text{-}3\sigma}$), the time for the maximum PDF of the center point of integral volume ($t_{\max\text{-PDF}}$), and the time for the maximum collision probability ($t_{\max\text{-prob}}$). The table also gives the values for safety obtained using the simulation method and the simplified method.

In Table 2, it is found that $t_{\min\text{-}d\text{-}3\sigma}$ is very close to $t_{\min\text{-}d\text{-center}}$ for points 1 and 2. Figure 3 illustrates the time history of the relative distance of the first three points, respectively. It is also found that the minimum 3σ ellipsoid distance of both points 1 and 2 are larger than

Table 1 Maneuver impulses (LVLH)

Impulses	1	2	3
t_i(s)	500	1500	3000
Δv_{ix}(m/s)	8.16061	−1.69676	2.44124
Δv_{iy}(m/s)	−0.923923	−1.66979	0.444352
Δv_{iz}(m/s)	−15.3841	−1.86493	−8.87236

Table 2 Safety properties of evaluation points

Evaluation point	1	2	3	4
$t_{\min\text{-}d\text{-center}}$	540 s	2850 s	1510 s	0–5200 s
$t_{\min\text{-}d\text{-}3\sigma}$	550 s	3020 s	1400–1640 s	0–5200 s
$t_{\max\text{-PDF}}$	——	——	1520 s	110 s
$t_{\max\text{-prob}}$	——	——	1500 s	80 s
$I_{\text{safe}}^{\text{TBD}}$ (simulation)	−16, 794.4	−563.23	0.00500328	0.004588
$I_{\text{safe}}^{\text{TBD}}$ (simplified)	−16, 795.9	−767.57	0.00603154	0.005687

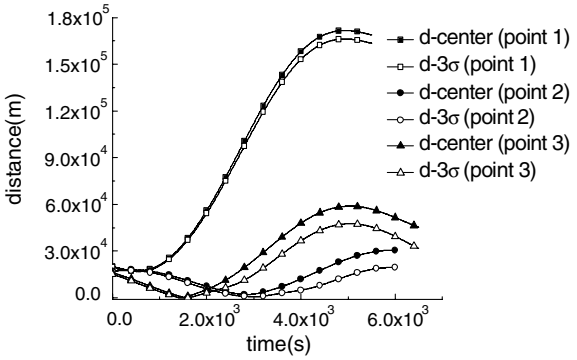

Fig. 3 Relative distance vs time.

zero; therefore, the safety performances of these two points are described by the minimum distance. And for point 3, evidently, the minimum 3σ ellipsoid distance is zero, so the safety performance of point 3 is denoted by the collision probability and the time history of the safety performance is plotted in Fig. 4. Furthermore, Fig. 4 demonstrates that the time history of PDF of point 3 is in accord with that of the collision probability. It also is seen from Table 2 that the $t_{\max\text{-PDF}}$ of point 3 is 1520 s, which is very close to the $t_{\max\text{-prob}}$ value of 1500 s. In this table, it is also found that the 3σ ellipsoid distance of point 4 is zero in the entire TBD time, so the safety performance is also denoted by the collision probability. In Fig. 4, it is seen that the time history of PDF is in accord with that of the collision probability.

From the last two rows of Table 2, it is found that $I_{\text{safe}}^{\text{TBD}}$ obtained using the simplified method is very close to that obtained using the simulation method. Moreover, in a computer with a CPU of 3 GHz and memory of 512 MB, the simulation method consumed 548.6 s, while the simplified method consumed 2.9 s, which is just 1/188 of that time.

It can be concluded that the simplified method offers almost the same degree of precision but achieves substantial savings in computer processing time. Furthermore, because in a Microsoft Visual C++ program environment, the proposed method can take less than 1 s to obtain the safety characteristic of one evaluation point, it can potentially be implemented in an onboard computer.

This safety performance can be used to evaluate the approach trajectory's safety with a failure mode such as thrusters ceasing, and it can be employed as another objective function in addition to the traditional performances of fuel cost and time of flight in designing an approach trajectory as used in [9–11].

C. Influence Factor Analysis

The rendezvous trajectory is mainly defined by the transfer time, number of impulses, and intervals between impulses. To demonstrate the characteristics of rendezvous trajectory safety, the influence of these main factors is analyzed. To this end, the transfer time was changed from 1000 to 9000 s; the number of impulses was set to 3, 4, 5, and 6; and the intervals between impulses were set as equal, increasing, and decreasing.

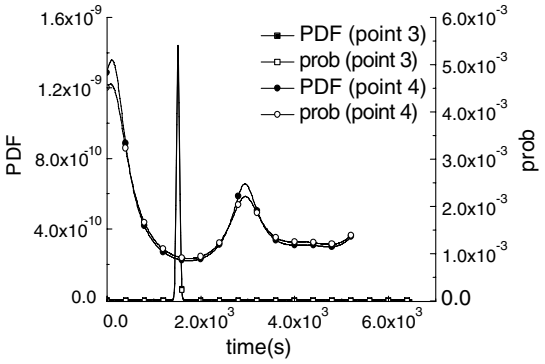

Fig. 4 Probability density function and collision probability vs time.

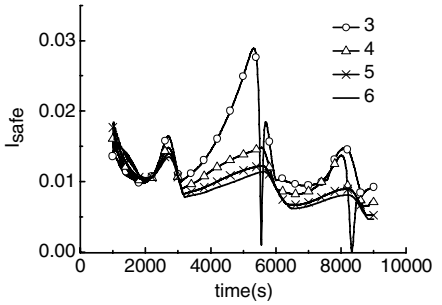

Fig. 5 I_{safe} vs transfer time and number of impulses.

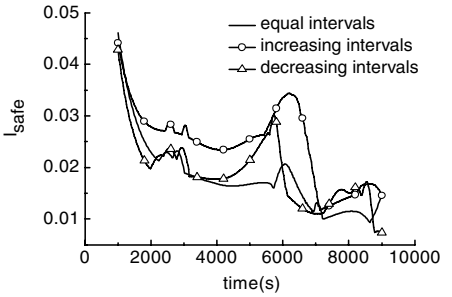

Fig. 6 I_{safe} vs interval of impulses.

Figure 5 illustrates the trend of I_{safe} in terms of the transfer time and the number of impulses. Generally speaking, the greater the number of impulses, the better the safety performance; as the transfer time increases, I_{safe} improves to a small degree. Figure 6 shows the relationship between I_{safe} and the interval between impulses, with the number of impulses fixed at five. No obvious relationship between I_{safe} and the interval between impulses can be seen in Fig. 6. Thus, for the design of rendezvous trajectories with safety as an objective function, emphasis should be placed on the transfer time and the number of impulses, with less attention given the interval between impulses.

VI. Conclusions

A quantitative performance index of safety for spacecraft rendezvous trajectories that considers both navigation and control errors is proposed. The simplified yet more efficient calculation methods for this performance index are presented. By considering an example of a homing rendezvous mission, the proposed performance index was demonstrated to be able to provide an exact evaluation of rendezvous trajectories with consideration of operational errors; the proposed performance analysis method can potentially be employed for in-orbit safety analysis. The main factors influencing the characteristic of trajectory safety were found to be the transfer time and the number of impulses, both of which should receive more attention than the interval between impulses during the design of safe rendezvous trajectories.

Acknowledgments

This work was supported by the National Natural Science Foundation of China (no. 10902121), the Postdoctoral Science Foundation of China (no. 20090450210), and the Science Project of the National University of Defense Technology (no. JC09-01-01).

References

[1] Fehse, W., *Automated Rendezvous and Docking of Spacecraft*, Cambridge Univ. Press, London, 2003, pp. 76–111, 141–144.

[2] Hechler, F., "Safe and Fuel Minimum Reference Trajectories for Closed Loop Controlled Approaches," *First European In-Orbit Operations Technology Symposium*, ESA, SP-272, Darmstadt, Germany, Nov. 1987, pp. 19–28.

[3] Eckstein, M. C., "Safe Rendezvous Approach to a Space Station by Impulsive Transfers and Continuous Thrust Arcs," *First European In-Orbit Operations Technology Symposium*, ESA, SP-272, Darmstadt, Germany, Nov. 1987, pp. 3–12.

[4] Roger, A. B., and McInnes, C. R., "Safety Constrained Free Flyer Path Planning at the International Space Station," *Journal of Guidance, Control, and Dynamics*, Vol. 23, No. 6, 2000, pp. 971–979. doi:10.2514/2.4656

[5] Jacobsen, S., Lee, C., Zhu, C., and Dubowsky, S., "Planning of Safe Kinematics Trajectories for Free-Flying Robots Approaching an Uncontrolled Spinning Satellite," *ASME 2002 Design Engineering Technical Conferences and Computer and Information in Engineering Conference*, Montreal, DETC 2002/MECH-34336, 2002.

[6] Matsumoto, S., Jacobsen, S., Dubowsky, S., and Ohkami, Y., "Approach Planning and Guidance for Uncontrolled Rotating Satellite Capture Considering Collision Avoidance," *7th International Symposium on Artificial Intelligence, Robotics and Automation in Space*, Nara, Japan, May 2003.

[7] Naasz, B., "Safety Ellipse Motion with Coarse Sun Angle Optimization," *595 Flight Mechanics Symposium*, NASA CP 2005-0241964, Greenbelt, MD, Oct. 2005.

[8] Breger, L., and How, J. P., "Safe Trajectories for Autonomous Rendezvous of Spacecraft," *Journal of Guidance, Control, and Dynamics*, Vol. 31, No. 5, 2008, pp. 1478–1489. doi:10.2514/1.29590

[9] Luo, Y. Z., Tang, G. J., and Lei, Y. J., "Optimal Multi-Objective Linearized Impulsive Rendezvous," *Journal of Guidance, Control, and Dynamics*, Vol. 30, No. 2, 2007, pp. 383–389. doi:10.2514/1.21433

[10] Luo, Y. Z., Lei, Y. J., and Tang, G. J., "Optimal Multi-Objective Nonlinear Impulsive Rendezvous," *Journal of Guidance, Control, and Dynamics*, Vol. 30, No. 4, 2007, pp. 994–1002. doi:10.2514/1.27910

[11] Luo, Y. Z., Tang, G. J., and Parks, G., "Multi-Objective Optimization of Perturbed Impulsive Rendezvous Trajectories Using Physical Programming," *Journal of Guidance, Control, and Dynamics*, Vol. 31, No. 6, 2008, pp. 1829–1832. doi:10.2514/1.35409

[12] Woodburn, J., and Tanygin, S., "Position Covariance Visualization," AIAA/AAS Astrodynamics Specialist Conference and Exhibit, Monterey, CA, AIAA Paper 2002-4985, Aug. 2002.

[13] Coppola, V., and Woodburn, J., "Determination of Close Approaches Based on Ellipsoidal Threat Volumes," *Advances in the Astronautical Sciences*, Vol. 102, 1999, pp. 1013–1024; alsoAAS/AIAA Space Flight Mechanics Meeting, Breckenridge, CO, American Astronomical Soc. Paper 99-170, Washington, D.C., Feb. 1999.

[14] Akella, M. R., and Alfriend, K. T., "Probability of Collision between Space Objects," *Journal of Guidance, Control, and Dynamics*, Vol. 23, No. 5, 2000, pp. 769–772. doi:10.2514/2.4611

[15] Wang, H., "Control and Trajectory Safety of Rendezvous and Docking," Ph.D. Thesis, National Univ. of Defense Technology, Changsha, PRC, 2007.